Stem Cell Reports
Report
ISSCR
OPEN ACCESS

Rapid Generation of Human Genetic Loss-of-Function iPSC Lines by Simultaneous Reprogramming and Gene Editing

Andrew M. Tidball,[1] Louis T. Dang,[2] Trevor W. Glenn,[1] Emma G. Kilbane,[1] Daniel J. Klarr,[1] Joshua L. Margolis,[1] Michael D. Uhler,[3,4] and Jack M. Parent[1,5,*]
[1]Department of Neurology, University of Michigan Medical School, 5021 BSRB, 109 Zina Pitcher Place, Ann Arbor, MI 48109-2200, USA
[2]Department of Pediatrics
[3]Department of Biological Chemistry
[4]Molecular and Behavioral Neuroscience Institute
University of Michigan Medical School, Ann Arbor, MI 48109, USA
[5]VA Ann Arbor HealthCare System, Ann Arbor, MI 48105, USA
*Correspondence: parent@umich.edu
http://dx.doi.org/10.1016/j.stemcr.2017.07.003

SUMMARY

Specifically ablating genes in human induced pluripotent stem cells (iPSCs) allows for studies of gene function as well as disease mechanisms in disorders caused by loss-of-function (LOF) mutations. While techniques exist for engineering such lines, we have developed and rigorously validated a method of simultaneous iPSC reprogramming while generating CRISPR/Cas9-dependent insertions/deletions (indels). This approach allows for the efficient and rapid formation of genetic LOF human disease cell models with isogenic controls. The rate of mutagenized lines was strikingly consistent across experiments targeting four different human epileptic encephalopathy genes and a metabolic enzyme-encoding gene, and was more efficient and consistent than using CRISPR gene editing of established iPSC lines. The ability of our streamlined method to reproducibly generate heterozygous and homozygous LOF iPSC lines with passage-matched isogenic controls in a single step provides for the rapid development of LOF disease models with ideal control lines, even in the absence of patient tissue.

INTRODUCTION

Two recent breakthroughs in biology have opened the door to rapid advances in biomedical research. The development of induced pluripotent stem cells (iPSCs) and gene editing using the clustered regularly interspersed short palindromic repeats (CRISPR) and CRISPR-associated 9 (Cas9) endonuclease system have brought patient-specific disease modeling to researchers interested in a wide variety of human disorders. As has been the gold standard in mouse models, the ideal system for *in vitro* disease modeling is to compare cells containing genomes that are isogenic except for the pathogenic mutation (Li et al., 2015; Smith et al., 2015). Despite advances in CRISPR-targeted mutagenesis and iPSC reprogramming, challenges remain for effectively combining these two technologies.

iPSCs are a rapidly dividing, expandable source of cells theoretically able to generate any cell type in the human body. However, these cells present multiple obstacles as a substrate for CRISPR gene editing. First, single clonal lines are difficult to generate from established iPSCs. Human iPSCs do not survive single-cell dissociation without the addition of a rho-associated coiled-coil kinase (ROCK) inhibitor (Watanabe et al., 2007). Moreover, single-cell plating into 96-well plates to generate clonal lines necessitates low-oxygen incubators and optimization of flow-cytometry parameters if cell sorting is required (Forsyth et al., 2006). Single-cell passaging of human iPSCs also has been shown to increase genomic abnormalities, which in turn increases the number of total clones needed to guarantee a fully validated line (Bai et al., 2014). Second, selectable markers are often introduced to overcome potential issues of heterogeneity after gene editing (Li et al., 2015; Smith et al., 2015). However, this introduction necessitates a homologous recombination event—a much less common process compared with non-homologous end-joining (NHEJ)—as well as designing a large cassette with long homology arms. Alternatively, NHEJ can be activated by simply introducing the CRISPR/Cas9 plasmid with an appropriate guide RNA (gRNA) (Sánchez-Rivera and Jacks, 2015). The resulting indels often cause frameshifts leading to loss-of-function (LOF) mutations, but the problems of single-cell clones and heterogeneous cultures arise once again. Third, undesired mutations or genomic abnormalities may occur with each cloning of a stem cell line; therefore, examination of multiple clones is needed, even with isogenic controls, to account for potential genetic changes.

To circumvent many of these problems, we generated iPSC lines using simultaneous reprogramming and CRISPR/Cas9 gene editing similarly to Howden et al. (2015), but with the more specific purpose of characterizing the efficiency, indel type, homogeneity, and gene function of mutated iPSC lines. We applied this approach to five human LOF disease genes, four that cause epileptic encephalopathy (EE) and one encoding a metabolic

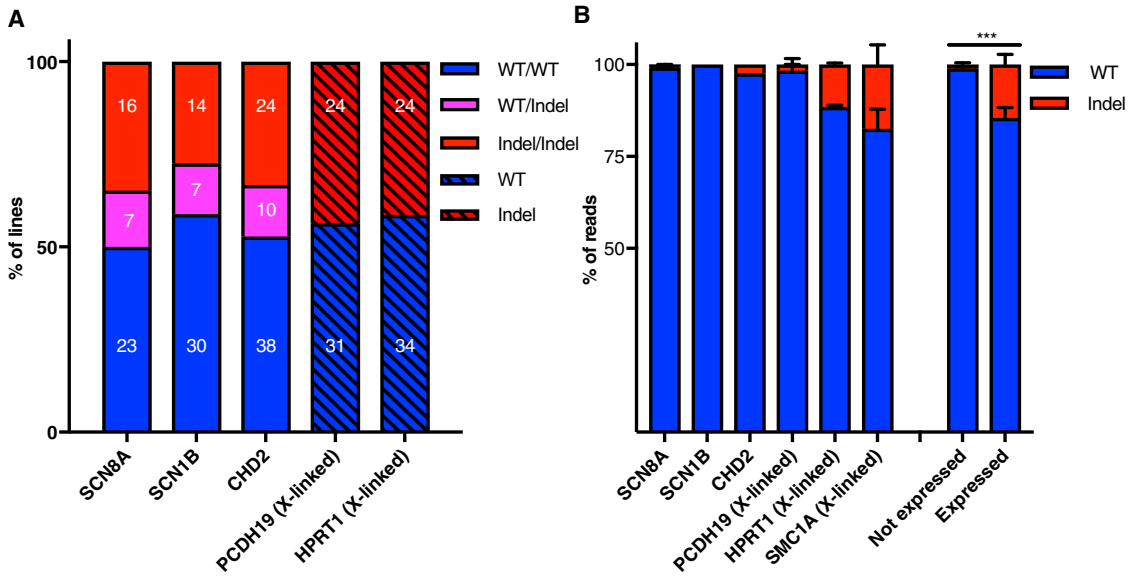

Figure 1. Reproducible Indel Formation Rate with Simultaneous Fibroblast CRISPR and Reprogramming to iPSC Lines

In eight separate experiments, fibroblasts were electroporated with plasmid reprogramming factors and a plasmid containing Cas9 and gRNA sequence. iPSCs were then isolated and sequenced over the CRISPR cut site.

(A) The percentage of lines for each genotype for the five CRISPR experiments is presented with the raw number of lines for each genotype superimposed on the bars.

(B) The percentages of wild-type (WT; unmutated) and indel (mutated) next-generation sequencing reads for established iPSC lines transfected with the same CRISPR plasmids as in (A). The genes were then binned as either known to be expressed or not expressed in iPSCs (see text for details). Error bars denote SEM. ***$p < 0.0001$ by t test.

enzyme, including both autosomal and X-linked genes. This method rapidly generated both LOF mutant and isogenic control iPSC lines in a single step. Additionally the clonal step inherent to the reprogramming process overcame one of the central hurdles in iPSC gene editing. The nearly even percentages for each genotype as well as the striking reproducibility between different genes and fibroblast lines necessitates minimal numbers of isolated clones, freeing time and resources for downstream disease-modeling assays.

RESULTS

Simultaneous Reprogramming and Gene Editing Results in Reproducible Numbers of LOF Lines

To generate knockout iPSC lines, we electroporated episomal reprogramming vectors into either human dermal fibroblasts or human foreskin fibroblasts (Okita et al., 2011). We simultaneously electroporated a CRISPR/Cas9 plasmid vector (1 μg) containing the gRNA sequence targeting one of five different genes: Voltage-Gated Sodium Channel (VGSC) alpha subunit 8 (*SCN8A*), Protocadherin-19 (*PCDH19*), VGSC beta 1 (*SCN1B*), Chromodomain Helicase DNA Binding Protein 2 (*CHD2*), and Hypoxanthine Phosphoribosyltransferase 1 (*HPRT1*). Mutations in the first four genes cause early infantile epileptic encephalopathies. Mutations in *HPRT1* lead to Lesch-Nyhan syndrome, a metabolic disorder affecting the nervous system and other organs. For each experiment we isolated 60–96 colonies and collected genomic DNA while continuing to propagate the lines. PCR and Sanger sequencing were used to assess indel formation in each of the iPSC lines. Between 46 and 72 iPSC lines (representing the numbers remaining from the original 96 wells; some clones did not survive isolation and expansion, while others did not yield sufficient DNA with the 96-well plate DNA isolation kit) for each of the five genes were successfully characterized as wild-type (WT) or indel for each allele (Figure 1A). Strikingly, the distribution of genotypes for the three autosomal genes (*SCN8A*, *SCN1B*, and *CHD2*) was not statistically different among the experiments (chi-square $p = 0.9239$), despite targeting three different genes in two different fibroblast lines (female dermal fibroblasts for *SCN8A* and *SCN1B*; foreskin fibroblasts for *CHD2*). Additionally, the X-linked genes (using a male foreskin fibroblast line) had a remarkably similar ratio of WT and indel lines (chi-square $p = 0.7941$). The percentage of non-mutated lines in each reprogramming was on average 55% ± 4% SD. These data indicate that the formation of knockout lines during

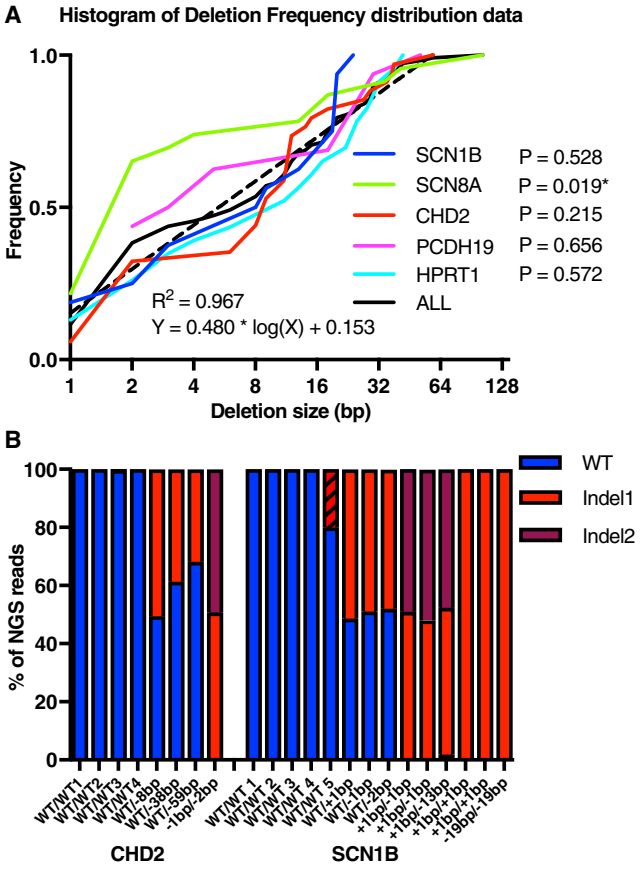

Figure 2. Indel Formation Fits a Log-Normal Distribution with Low Rate of Genotype Heterogeneity

(A) The sizes for all wild-type (WT) Cas9 deletion mutation clones are plotted as a cumulative frequency distribution and fitted to a log-linear curve (n = 112). The p value indicates the significance calculated comparing the individual line with all other lines by the Mann-Whitney test.

(B) *CHD2* and *SCN1B* fibroblasts undergoing simultaneous CRISPR and reprogramming to iPSC lines were tested for genotype heterogeneity by deep sequencing of the PCR product with primers flanking the Cas9 cut site. Only one line (*SCN1B* WT/WT 5) was found to be heterogeneous with 20% of the PCR product containing a 1-bp deletion. A compound heterozygous mutant line (*SCN1B* +1 bp/−13 bp) had low-level WT contamination (1.9%), which is too small to be seen on the graph. Two *CHD2* lines deviated from a 1:1 ratio due to a technical bias against smaller constructs, which resulted from large deletion sizes (−38 and −59 bp).

reprogramming is reproducible, irrespective of the individual gene targeted.

Comparison with CRISPR Indel Formation in Established iPSCs

To test whether this reproducibility was a product of our methodology or inherent to the genes and gRNAs tested, we performed direct CRISPR gene editing in established human iPSC lines. We transfected two established clonal iPSC lines from foreskin fibroblasts with each of the CRISPR plasmids separately targeting the same five genes. Three days after transfection the cells were lysed and genomic DNA was collected. The targeted genomic region for each CRISPR gRNA was amplified by PCR and sent for next-generation sequencing (>20,000 read depth per sample). The resulting reads were binned by percent as WT (unmutated) or mutated (Figure 1B). The four epilepsy genes had an extremely low level of mutations (~1%); however, *HPRT1* was mutated at a much higher rate (11.5%). Interestingly, based on a database of iPSC expression data, of the five genes only *HPRT1* is significantly expressed in human PSCs (Mallon et al., 2013). To test the hypothesis that the active state resulted in greater mutagenesis, we performed the same experiment using a gRNA for *SMC1A*, a part of the cohesin complex. Heterozygous LOF mutations in *SMC1A* have recently been correlated with severe epilepsy (Symonds et al., 2017). Furthermore, *SMC1A* is highly expressed in iPSCs (Mallon et al., 2013). The mutation rate in *SMC1A* was even greater than *HPRT1* with 17.5% of the PCR products harboring indel mutations. Therefore, actively transcribed genes were mutated at a significantly higher rate than inactive genes ($p < 0.0001$ by t test). These data indicate an increased Cas9 efficiency in actively transcribed genes for gene editing in established stem cell lines, while the higher efficiency and reproducibility seen in the combined reprogramming with CRISPR gene editing suggests that the reprogramming process may alleviate these differences.

We further characterized each indel formed in the combined reprogramming experiments (see Table S2). The vast majority of these mutations (72%, 81/112 mutations) are predicted to result in a frameshift that introduces a premature stop codon. As commonly seen with NHEJ-dependent indels, the deletions in the iPSC lines tended to be small (50% of deletions <6 bp). A cumulative size-distribution plot of the 112 deletions fit a log-normal distribution (Figure 2A) with an R^2 value of 0.967. Our deletion data were nearly identical to those seen previously for the distribution of deletion size using non-LTR retrotransposable elements in *Drosophila* used as a model of random mutagenesis (Ptak and Petrov, 2002). Statistical analysis showed that only the *SCN8A* experiment significantly deviated from this distribution due to an increased propensity for 2-bp deletions possibly related to the cut site occurring in the middle of a 2-bp repeat (CACA). Of note, the fitted line (Figure 2A) indicates that 99% of all deletion mutations will be less than 55 bp, suggesting that this is the minimum distance that should be used from the end of the sequencing primers to the CRISPR cut site. This is

important because large mutations that include part of the sequencing primer site will not be amplified and will subsequently be missed during sequencing. Additionally, we have characterized the indels formed by the direct iPSC transfection (see Table S2).

Validating LOF iPSC Line Genotype Homogeneity, Genomic Stability, and gRNA Off-Target Sites

Homogeneous iPSC colonies are necessary in order to use knockout lines generated by simultaneous CRISPR and reprogramming for disease modeling. We therefore tested whether the genotypes were heterogeneous. To this end, we used deep sequencing (>20,000× read depth) of our PCR amplified products over the cut site from the *CHD2* and *SCN1B* lines and quantified the percentage of each DNA species (Figure 2B). All sequenced *CHD2* lines were homogeneous, having the species expected from the original genotyping in the correct ratio (Figure 2B, left). Note that a technical bias yielded a smaller percentage of reads for shorter sequences, thus causing the disparity in the large deletions for *CHD2* (−38 and −59 bp). For the *SCN1B* set (Figure 2B, right), one WT/WT line showed 20% contamination of a T-insertion mutation. This finding likely reflected one WT/WT and one WT/indel line growing together prior to colony isolation. Additionally, one heterozygous knockout line had 1.9% WT contamination. This level of WT product was probably a result of DNA contamination rather than true heterogeneity. Therefore, we found only one clearly heterogeneous line out of 22 clones analyzed. Furthermore, we identified heterogeneous (WT and mutant) DNA in the sequences of only two out of 60 *HPRT1* knockout iPSC lines despite only a single allele (X chromosome in a male line). In total, we observed ~3.6% heterogeneous lines, likely resulting from two iPSC colonies growing closely together and being isolated simultaneously.

Additional characterization using an SNP chip microarray (17 lines) and/or g-band karyotyping (8 lines; 3 unique) revealed only one large chromosomal abnormality (inv(9)(p11q13)) out of the 20 total iPSC lines (including lines from each genotype class and from three different targeted genes). These data are summarized in Table S3. CRISPR off-target mutations are also a potential concern for this method. For this reason, we performed PCR on pooled genomic DNA samples from eight *CHD2* and ten *SCN1B* lines for the top exonic off-target sites predicted by the MIT CRISPR design tool (crispr.mit.edu), one for *CHD2*, and four for *SCN1B*. Deep sequencing of the PCR products from these pooled samples still provides 2,000× read depth for each sample (for primer sequences, see Table S1). From these data, we found no mutated species for either pooled sample at any of the off-target sites (data not shown).

All Indels in the *HPRT1* Gene Result in Confirmed LOF

We next sought to demonstrate LOF of a targeted gene product to validate our methodology. Unfortunately, many of the genes we mutated are only expressed in mature neurons or do not have reliable antibodies. Therefore, we designed an experiment to test for LOF in a large number of clonal lines and correlate the function with each indel. To this end, we used our simultaneous CRISPR and reprogramming strategy to generate iPSC lines with mutations in the *HPRT1* gene in which LOF causes Lesch-Nyhan syndrome. This enzyme-encoding gene on the X chromosome is dispensable in stem cell culture, but clones with *HPRT1* LOF become resistant to 6-thioguanine (6-TG) toxicity. We used this assay to test the function of each clone generated and compared the data with the sequencing results for *HPRT1*. The iPSC colonies were Sanger sequenced, and the resistance to 6-TG was measured after a 48-hr exposure to 30 μM 6-TG followed by a cell viability assay. The mean viability (treated/untreated) for all mutants was 99%, indicating the ineffectiveness of the 6-TG, while the mean for WT was 54% (Figure 3A). This ratio was only slightly higher than the 11 control iPSC lines generated by reprogramming without the Cas9 plasmid (39%). There was also no linear regression correlation between the size of the indel and the mean viability (R^2 = 0.054) with a slope of −0.003. To more precisely discriminate survival between WT and mutant lines, we fitted the data to a receiver-operating characteristic (ROC) curve (Figure 3B). At an optimal ratio of 76% (dotted line in Figure 3A), close to the midpoint between the two mean ratios (77%), we found two false positives and one false negative. The mutation in the false positive (53% viability), which may reflect a mutation that does not lead to LOF, was a 2-bp deletion identical to another clone, which had 95% viability. Therefore, we believe this value is experimental error not associated with retained gene function, and all other mutant lines demonstrated clear LOF. Interestingly, in-frame mutations, which could theoretically retain function, had a mean viability of 99% while two heterogeneous lines (mixed WT and mutant) had a mean viability nearly identical to the discrimination threshold (77%).

DISCUSSION

We have designed and verified a clearly defined protocol for reproducibly generating both heterozygous and homozygous LOF mutations in isogenic iPSC lines. The reproducibility across five different previously unvalidated gRNAs for genes throughout the genome is truly remarkable in the CRISPR field. Typically, Cas9 has reduced density and diffusion in heterochromatic regions, which would likely

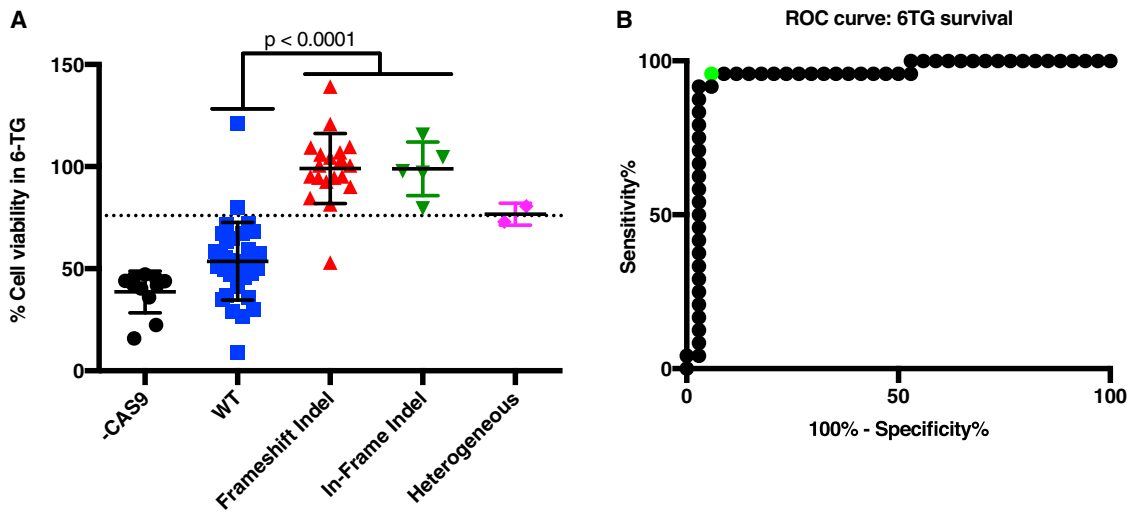

Figure 3. Confirming LOF in Mutant iPSC Lines

(A) Fibroblasts that underwent simultaneous *HPRT1* CRISPR and iPSC reprogramming were treated with 6-TG (genotype was determined after survival analysis), and percent viability was calculated by determining the CellTiter Blue signal ratio between 6-TG-treated and -untreated cells. The −Cas9 cells were 6-TG-treated iPSC lines generated in parallel without the *HPRT1* CRISPR plasmid. Statistical analysis between wild-type (WT) and indel lines was performed by t test. Error bars denote SD. The number of clones for each group in the graph are n = 11, 35, 19, 5, and 2, respectively.

(B) A ROC curve was generated from the WT and indel lines (frameshift and in-frame) to choose the ideal discrimination value for the assay (76%, depicted as the green point on the ROC curve and as the dotted line in panel A). The two heterogeneous lines were found to have both WT and mutant sequence despite *HPRT1* being on the X chromosome in male cell lines.

result in reduced efficiency of gRNAs targeting Cas9 to compact chromatin structures (Knight et al., 2015). However, in the context of early reprogramming, the fibroblasts are undergoing rapid chromatin remodeling as the reprogramming factors access silenced intermediate and pluripotency genes (Apostolou and Hochedlinger, 2013). Furthermore, off-target binding of CAS9 to seed sequence sites directly correlates with DNase I hypersensitivity sequences and inversely correlates with CpG methylation sites, indicating reduced targeting to inactive, methylated DNA sequences (Kuscu et al., 2014; Wu et al., 2014). The difference in CRISPR indel formation in established iPSC lines compared with our combined approach further supports the hypothesis that reprogramming allows Cas9 better access to some genes in inactive chromatin. Therefore, combining reprogramming and CRISPR/Cas9 genome editing is likely to provide a means to efficiently target regions of the genome that have previously been difficult to mutate or edit. Additionally, when the Cas9 protein is engineered to degrade in G_1 of the cell cycle, the indel formation rate for combined CRISPR and reprogramming is drastically reduced (Howden et al., 2016). These differences are likely due to the cell-cycle phase-specific disparities in DNA repair pathways found in human fibroblasts (Mao et al., 2008). Given the greater percentage of somatic cells, including fibroblasts, in G_0/G_1 compared with PSCs, these differences may account for the high level of indel formation in our method.

While combining CRISPR gene editing and iPSC reprogramming into a single electroporation step was first demonstrated by Howden et al. (2015), we have significantly defined, validated, and expanded upon their original work. We also highlight the particular utility of our protocol for LOF disease modeling because of efficient production of WT, heterozygous, and homozygous LOF lines in a single step. Additionally the high rate of mutagenized lines allows for multiplexing gRNAs to mutate multiple genes simultaneously, although testing this possibility is beyond the scope of the current study. In short, our streamlined method overcomes many of the shortcomings of LOF gene editing in iPSCs, allowing for rapid production of well-controlled iPSC disease models for investigating hemizygous and recessive LOF disease mechanisms.

EXPERIMENTAL PROCEDURES

gRNA Design and px330 Annealing

The gRNAs were designed using the MIT CRISPR design tool (crispr.mit.edu) to target exon 1 or another early exon not known to be alternatively spliced such that a frameshift would result in complete LOF. Forward and reverse oligos with the appropriate 5′ overhang were obtained (Life Tech). The annealed oligo duplex was

ligated with T4 ligase into the px330 (WT Cas9) plasmid (addgene.org) previously digested with BbsI (NEB). For gRNA sequences, see Table S1.

Primer Design

Sequencing PCR primers were designed to amplify a 200- to 250-bp product nearly evenly flanking the CRISPR/Cas9 cut site. After kit PCR purification (Qiagen), this product was used for Sanger sequencing to identify the indels formed and for next-generation sequencing to identify all PCR products and abundance. For primer sequences, see Table S1.

Fibroblast and iPSC Culture

Foreskin fibroblasts were obtained from MT-Globalstem. Dermal fibroblasts were obtained from a female individual with no known genetic disorders with consent obtained under a protocol approved by the Institutional Review Board of the University of Michigan Medical Center. These cells were maintained in DMEM with 10% fetal bovine serum, non-essential amino acids, and penicillin/streptomycin. Medium was exchanged every 2–3 days. Subconfluent fibroblasts were passaged with trypsin. iPSC lines were maintained on Matrigel-coated dishes in mTeSR1 medium, exchanged daily. When cultures reached ~40% confluence, they were passaged using dispase and replated at a 1:4 to 1:8 dilution as small clumps using dispase.

iPSC Reprogramming

Fibroblasts (1×10^5) between passages 5 and 10 were electroporated in Neon electroporation kit reagent R premixed with reprogramming plasmids (1 μg each of pCXLE-hOCT3/4-p53shRNA, pCXLE-hUL, and pCXLE-hSK) using the Neon Transfection system (Thermo Fisher) with 3 pulses of 1,650 V for 10 ms each as previously published (Okita et al., 2011) with or without the addition of 1 μg CRISPR/Cas9 plasmid (px330 or px335; addgene.org). Fibroblasts ($4–20 \times 10^3$) were then plated into each well of a Matrigel-coated 6-well plate in fibroblast growth medium. The fibroblast growth medium was changed the following day. Three days after electroporation, medium was changed to TeSR-E7 (STEMCELL Technologies) and replaced daily.

iPSC Colony Isolation, 96-Well Plate Passaging, and Genomic DNA Isolation

iPSC colonies appeared 14–21 days after electroporation. Special care was taken to isolate small circular colonies with no indication of multiple clones merging to reduce the probability of heterogeneous genotypes. If the fibroblasts are confluent, the shape of iPSC colonies may look suboptimal; however, after manual isolation the colony morphology improves. Colonies were isolated using a P200 micropipette under an inverted HEPA workstation and transferred into a Matrigel-coated 96-well plate containing 100 μL of mTeSR1 with 10 μM ROCK inhibitor (Y27632; Tocris). The next day the medium was changed to mTeSR1 without Y27632 and replaced daily thereafter. When isolated colonies reached an average confluence of ~40%, cells were passaged as follows. The 96-well plate was washed once (Ca^{2+}/Mg^{2+}-free PBS, room temperature) followed by a 5-min incubation with 30 μL of Accutase per well at 37°C. Then 210 μL of mTesr1 medium containing 10 μM Y27632 was pipetted into each well, cells were mixed by gently pipetting once, and 50 μL of medium was transferred from each well to a new Matrigel-coated 96-well plate. An extra 100 μL of mTeSR1 medium with 10 μM Y27632 was added to each well to further dilute the Accutase. Cells were passaged every 3–4 days when a large percentage of wells were ~100% confluent. Genomic DNA was isolated using the ZR-96 Quick-gDNA Kit (Zymo Research).

Sanger Sequencing and CRISPR Deep Sequencing

Genomic DNA was extracted from either a 96-well plate as described above or, for confirmation analysis, DNA was extracted from one well of a 6-well plate (~50% confluent) using the DNeasy genomic isolation kit (Qiagen). For Sanger sequencing, PCR reactions (25 μL) were run with 0.4 μM of each primer with 2× GoTaq master mix, and 5–15 ng from the 96-well plate extractions or 25–100 ng of genomic DNA from DNeasy preparations. The resulting PCR product was then purified using the ZR-96 DNA Clean-up kit (Zymo Research) or the PCR product purification kit (Qiagen). PCR products were submitted to the University of Michigan Sequencing Core for Sanger sequencing. CRISPR deep sequencing of the same PCR products was performed by the CCIB DNA Core Facility at Massachusetts General Hospital (Cambridge, MA).

SNP Chip Microarray and g-Band Karyotyping

Genomic DNA samples were generated from iPSC lines as described above. These samples were submitted to the University of Michigan Sequencing Core. A HumanCoreExome-24 v1.1 Infinium Whole genome genotyping BeadArray (Illumina) was performed on these samples and analyzed for copy-number variations (CNVs) using KaryoStudio software (Illumina). While a few possible small CNVs (0.15–0.29 MB) with low confidence scores (50–100 [KaryoStudio]) were identified in the original fibroblast lines and subsequently generated iPSC lines, in all 17 iPSC lines analyzed no unique abnormalities arose. iPSC lines were also submitted for standard g-band karyotype analysis to Cell Guidance Systems. For each line, 20 metaphase spreads were analyzed. Of the eight lines tested, one had a chromosomal abnormality in all cells: inv(9)(p11q13). These data are summarized in Table S3.

6-Thioguanine Assay

A 96-well plate of iPSC colonies was passaged onto two 96-well Matrigel-coated plates as above. For the next 2 days the medium was changed to mTeSR1 with or without 30 μM 6-TG. When most of the control wells were confluent, the medium was replaced with 100 μL of mTeSR1 and 20 μL of CellTiter Blue Viability reagent. After a 1-hr incubation, fluorescence intensity was determined (excitation 570 nm; emission 595 nm) on a DTX 880 Multimode Detector (Beckman Coulter). The fluorescence signal from an empty well was used for background subtraction from all measurements, and percent survival was determined by dividing the 6-TG signal by the untreated signal in the parallel plate.

Statistical Methods

All statistical analyses were performed using Prism 7 (GraphPad). Error bars, significance values, and statistical tests are detailed in the figure legends.

SUPPLEMENTAL INFORMATION

Supplemental Information includes three tables and can be found with this article online at http://dx.doi.org/10.1016/j.stemcr.2017.07.003.

AUTHOR CONTRIBUTIONS

Study concept and design, A.M.T., L.T.D., M.D.U., and J.M.P. Acquisition of data, A.M.T., L.T.D., T.W.G., E.G.K., D.J.K., and J.L.M. Analysis and interpretation of data, A.M.T. and L.T.D. Drafting of manuscript, A.M.T. and J.M.P. Critical revision, A.M.T., L.T.D., M.D.U., and J.M.P.

ACKNOWLEDGMENTS

This work was supported by grants from the NIH NS090364 and Citizens United for Research in Epilepsy (CURE) to J.M.P. We thank the Center for Computational and Integrative Biology (CCIB) DNA Core Facility at Massachusetts General Hospital (Cambridge, MA) for providing sequencing services.

Received: February 3, 2017
Revised: July 3, 2017
Accepted: July 4, 2017
Published: August 3, 2017

REFERENCES

Apostolou, E., and Hochedlinger, K. (2013). Chromatin dynamics during cellular reprogramming. Nature *502*, 462–471.

Bai, Q., Ramirez, J.-M., Becker, F., Pantesco, V., Lavabre-Bertrand, T., Hovatta, O., Lemaître, J.-M., Pellestor, F., and De Vos, J. (2014). Temporal analysis of genome alterations induced by single-cell passaging in human embryonic stem cells. Stem Cells Dev. *24*, 653–662.

Forsyth, N.R., Musio, A., Vezzoni, P., Simpson, A.H.R., Noble, B.S., and McWhir, J. (2006). Physiologic oxygen enhances human embryonic stem cell clonal recovery and reduces chromosomal abnormalities. Cloning Stem Cells *8*, 16–23.

Howden, S.E., Maufort, J.P., Duffin, B.M., Elefanty, A.G., Stanley, E.G., and Thomson, J.A. (2015). Simultaneous reprogramming and gene correction of patient fibroblasts. Stem Cell Reports *5*, 1109–1118.

Howden, S.E., McColl, B., Glaser, A., Vadolas, J., Petrou, S., Little, M.H., Elefanty, A.G., and Stanley, E.G. (2016). A Cas9 variant for efficient generation of indel-free knockin or gene-corrected human pluripotent stem cells. Stem Cell Reports *7*, 508–517.

Knight, S.C., Xie, L., Deng, W., Guglielmi, B., Witkowsky, L.B., Bosanac, L., Zhang, E.T., El Beheiry, M., Masson, J.-B., and Dahan, M. (2015). Dynamics of CRISPR-Cas9 genome interrogation in living cells. Science *350*, 823–826.

Kuscu, C., Arslan, S., Singh, R., Thorpe, J., and Adli, M. (2014). Genome-wide analysis reveals characteristics of off-target sites bound by the Cas9 endonuclease. Nat. Biotechnol. *32*, 677–683.

Li, H.L., Fujimoto, N., Sasakawa, N., Shirai, S., Ohkame, T., Sakuma, T., Tanaka, M., Amano, N., Watanabe, A., and Sakurai, H. (2015). Precise correction of the dystrophin gene in duchenne muscular dystrophy patient induced pluripotent stem cells by TALEN and CRISPR-Cas9. Stem Cell Reports *4*, 143–154.

Mallon, B.S., Chenoweth, J.G., Johnson, K.R., Hamilton, R.S., Tesar, P.J., Yavatkar, A.S., Tyson, L.J., Park, K., Chen, K.G., and Fann, Y.C. (2013). StemCellDB: the human pluripotent stem cell database at the National Institutes of Health. Stem Cell Res. *10*, 57–66.

Mao, Z., Bozzella, M., Seluanov, A., and Gorbunova, V. (2008). DNA repair by nonhomologous end joining and homologous recombination during cell cycle in human cells. Cell Cycle *7*, 2902–2906.

Okita, K., Matsumura, Y., Sato, Y., Okada, A., Morizane, A., Okamoto, S., Hong, H., Nakagawa, M., Tanabe, K., Tezuka, K., et al. (2011). A more efficient method to generate integration-free human iPS cells. Nat. Methods *8*, 409–412.

Ptak, S.E., and Petrov, D.A. (2002). How intron splicing affects the deletion and insertion profile in *Drosophila melanogaster*. Genetics *162*, 1233–1244.

Sánchez-Rivera, F.J., and Jacks, T. (2015). Applications of the CRISPR-Cas9 system in cancer biology. Nat. Rev. Cancer *15*, 387–395.

Smith, C., Abalde-Atristain, L., He, C., Brodsky, B.R., Braunstein, E.M., Chaudhari, P., Jang, Y.-Y., Cheng, L., and Ye, Z. (2015). Efficient and allele-specific genome editing of disease loci in human iPSCs. Mol. Ther. *23*, 570–577.

Symonds, J.D., Joss, S., Metcalfe, K.A., Somarathi, S., Cruden, J., Devlin, A.M., Donaldson, A., DiDonato, N., Fitzpatrick, D., and Kaiser, F.J. (2017). Heterozygous truncation mutations of the SMC1A gene cause a severe early onset epilepsy with cluster seizures in females: detailed phenotyping of 10 new cases. Epilepsia *58*, 565–575.

Watanabe, K., Ueno, M., Kamiya, D., Nishiyama, A., Matsumura, M., Wataya, T., Takahashi, J.B., Nishikawa, S., Nishikawa, S., Muguruma, K., and Sasai, Y. (2007). A ROCK inhibitor permits survival of dissociated human embryonic stem cells. Nat. Biotechnol. *25*, 681–686.

Wu, X., Scott, D.A., Kriz, A.J., Chiu, A.C., Hsu, P.D., Dadon, D.B., Cheng, A.W., Trevino, A.E., Konermann, S., and Chen, S. (2014). Genome-wide binding of the CRISPR endonuclease Cas9 in mammalian cells. Nat. Biotechnol. *32*, 670–676.